



Research Article

Micropyramid Vertical Ultraviolet GaN/AlGaN Multiple Quantum Wells LEDs on Si(111)

Yuebo Liu ¹, Honghui Liu,¹ Hang Yang,¹ Wanqing Yao,¹ Fengge Wang,¹ Yuan Ren,¹ Junyu Shen,¹ Minjie Zhang,¹ Zhisheng Wu,^{1,2} Yang Liu,^{1,2} and Baijun Zhang ^{1,2}

¹State Key Laboratory of Optoelectronic Materials and Technologies, Sun Yat-sen University, Guangzhou 510275, China

²School of Electronics and Information Technology, Sun Yat-sen University, 510006 Guangzhou, China

Correspondence should be addressed to Baijun Zhang; zhbajj@mail.sysu.edu.cn

Received 10 March 2021; Accepted 21 April 2021; Published 28 April 2021

Academic Editor: Shuyuan Xiao

Copyright © 2021 Yuebo Liu et al. This is an open access article distributed under the Creative Commons Attribution License, which permits unrestricted use, distribution, and reproduction in any medium, provided the original work is properly cited.

Micropyramid vertical GaN-based ultraviolet (UV) light-emitting diodes (LEDs) on Si(111) substrate have been fabricated by selective area growth to reduce threading dislocations and the polarization effects. There is no-light emission at the bottom and six planes of the pyramid at lower current due to the leakage current and nonradiative recombination of the dislocation at the bottom and the 90° threading dislocations (TDs) at six planes of the pyramid, and the top of the pyramid is the high-brightness region. The micropyramid UV LED has a high optical output intensity under a small current injection, and the series resistance of unit area is only a quarter of the conventional vertical LEDs, so the micropyramid UV LED would have a high output power under the drive circuit. The reverse leakage current of a single micropyramid UV LED is 2 nA at -10 V.

1. Introduction

The III nitride-based light-emitting diodes (LEDs) have been paid extensive attention thanks to their potential applications such as solid-state lighting, communication, sterilization, disinfection, water or air purification, and biochemistry [1–7]. The GaN-based LEDs cover range the ultraviolet (UV), entire visible-light and near-infrared spectrum (6.2 eV ~ 0.7 eV), due to the different composition of indium or aluminium [2]. The marketization of GaN-based visible LEDs has been replaced by AlGaN UV LEDs as the next research hotspot. At present, heteroepitaxial technology is the adopted method for the fabrication of AlGaN UV LEDs by metal-organic chemical vapor deposition (MOCVD) system, but as a high-temperature heteroepitaxial method, it has problems of the lattice and thermal mismatch [2, 8, 9]. The high density of threading dislocations (TDs) in epitaxial layer is attributed to the material parameters step in interface [10]. Nonradiative recombination centers in TDs reduce the internal quantum efficiency (IQE), which evolves into thermal centers of

damage the UV LEDs [8]. For lower TDs, two-step growth processes of predeposition AlN/AlGaN and selective area growth (SAG) were proposed [10]. Due to developments in crystal growth, chip processing, and packaging technologies, the external quantum efficiency (EQE) of NUV-LEDs of 365 nm, 385 nm, and 405 nm reaches 30%, 50%, and 60%, respectively [6]. However, the polarization effect of spacial separation of electron-hole wave function also greatly affects the IQE of LEDs [11]. The nonpolar plane reduces quantum-confined Stark effect (QCSE) from the spontaneous and piezoelectric polarization [12, 13]. Zhao et al. achieved IQE as high as 39% at 279 nm in a-plane AlGaN-based multiple quantum wells (MQWs) [14]. With the rapid development of crystal growth and the improvement of semiconductor manufacturing processes, micropyramid GaN-based UV LEDs on Si (111) can improve the EQE by SAG, which is ascribed to (1) high GaN crystal quality of lateral-growth [15], (2) semipolar plane of pyramid structure [12], and (3) larger emitting area of six planes of the pyramid. However, its related research work is rarely reported, especially single electrically driven GaN-based UV LED.

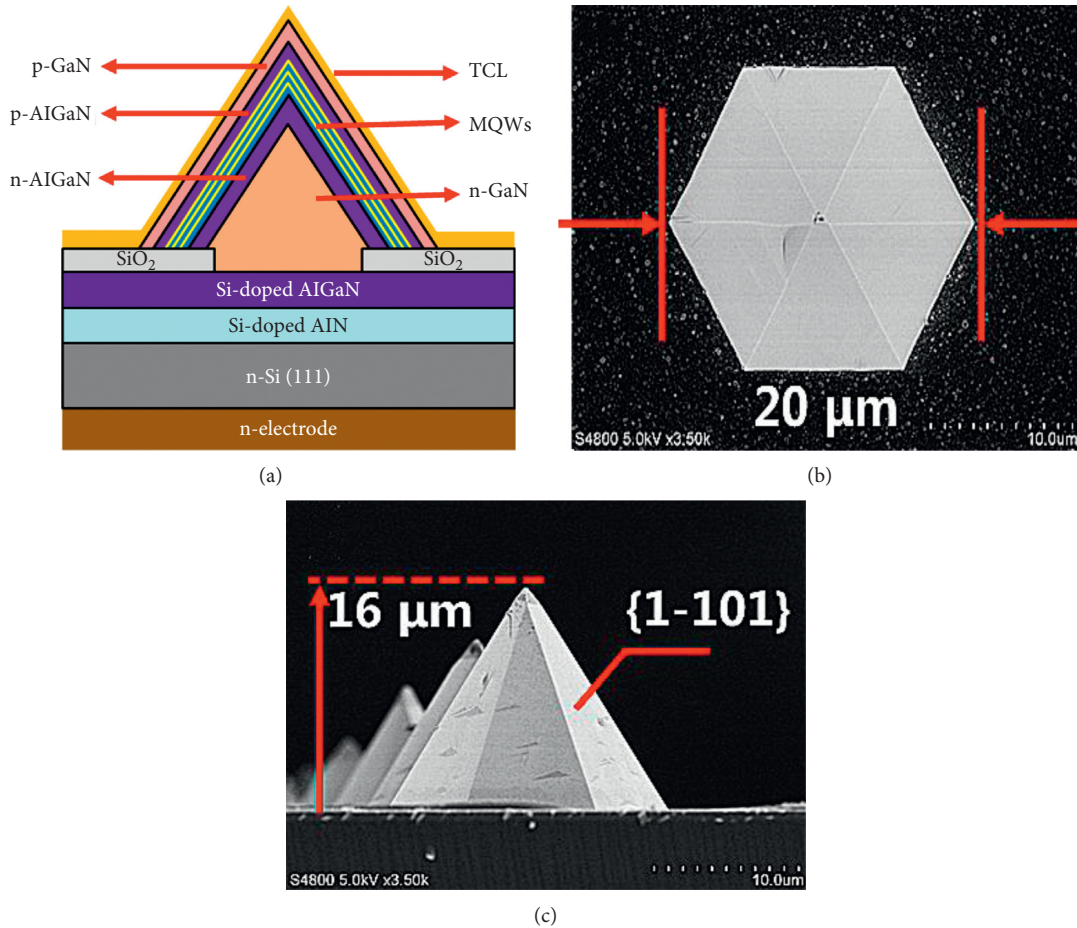


FIGURE 1: (a) Schematic diagram of the structure. (b) Top view and (c) front view SEM images of micro pyramid UV LED of no-electrode.

Hence, in this work, micro pyramid vertical GaN-based UV LED on Si (111) substrate has been fabricated by selective area growth. Six semipolar planes at the top of the pyramid greatly improve EQE due to lower the TDs and the lower polarization effects. The micro pyramid UV LED has a high optical output intensity under a small current injection, and the series resistance of unit area is only a quarter of the conventional vertical LEDs. With features such as these, the micro pyramid UV LED can be used as a subminiature UV light source, and it would have a high output power. The reverse leakage current of single electrically driven micro pyramid UV LED is 2 nA at -10 V. The top of the micro pyramid vertical GaN-based UV LED is a high-brightness region. However, the planes and bottom of the pyramid do not emit light due to leakage current, nonradiative recombination of the dislocation at the bottom, and the 90° TDs at six planes of the pyramid.

2. Experiments

Micro pyramid UV LED growth was performed on 2 inch Si(111) by SAG in a low-pressure MOCVD system. Vertical structure was designed to reduce current crowding, as shown in Figure 1(a). The resistivity of n-type Si is less than $0.02 \Omega\text{-cm}$. Before epitaxial growth, to remove impurities and oxides on the Si(111) plane, the n-type Si was

sequentially cleaned with $\text{H}_2\text{SO}_4:\text{H}_2\text{O}_2:\text{H}_2\text{O} = 3:1:1$, acetone solution, and isopropyl alcohol solution, respectively. A $\sim 50/1000$ nm thick n-AlGaN/AlN:Si film was grown on the Si substrate at 1095°C . Subsequently, a 100 nm thick amorphous SiO₂ layer was deposited on the AlGaN/AlN/Si by plasma-enhanced chemical vapor deposition (PECVD). Afterward, the mask of SiO₂ of $5.0\text{-}\mu\text{m}$ -diameter window openings with a $60\text{-}\mu\text{m}$ period was designed by wet-etching ($\text{HF}:\text{H}_2\text{O} = 1:10$). After cleaning, SiO₂/AlGaN/AlN/Si was again used in epitaxial grown for n-type GaN-based micro pyramid. The growth of GaN in the SAG of the window area belonged in secondary epitaxy, and the GaN rapidly grew on the window since the window of the patterned SiO₂ mask exposes the AlGaN layer. Ga atoms did not stay on the amorphous SiO₂ mask due to high-temperature decomposition of Ga-O and the larger nucleation energy of heteroepitaxy. However, Ga atoms migrated laterally to the window area for lateral growth, eventually healed into a point on top and formed the n-type GaN-based pyramid structure. Three pairs of AlGaN/GaN MQWs were grown on the six semipolar planes $\{1\bar{1}01\}$ of the pyramid, and then the p-type AlGaN/GaN:Mg was grown. The elements of Ga, Al, and N were provided by trimethyl-gallium (TMGa) or triethyl-gallium (TEGa), trimethyl-aluminum (TMAl), and ammonia (NH₃), respectively.

TABLE 1: The growth condition of the micropyramid LED in window areas.

	TMGa (sccm)	TMAI (sccm)	TEGa (sccm)	Pressure (mBar)	Temperature (°C)	Time (min)
n-GaN	40	—	—	300	1095	20
n-AlGaN	40	10	—	100	1100	10
AlGaN barrier	—	10	170	200	880	5
GaN well	—	—	340	200	800	2
p-AlGaN	—	10	210	200	980	8
p-GaN	—	—	210	200	980	4

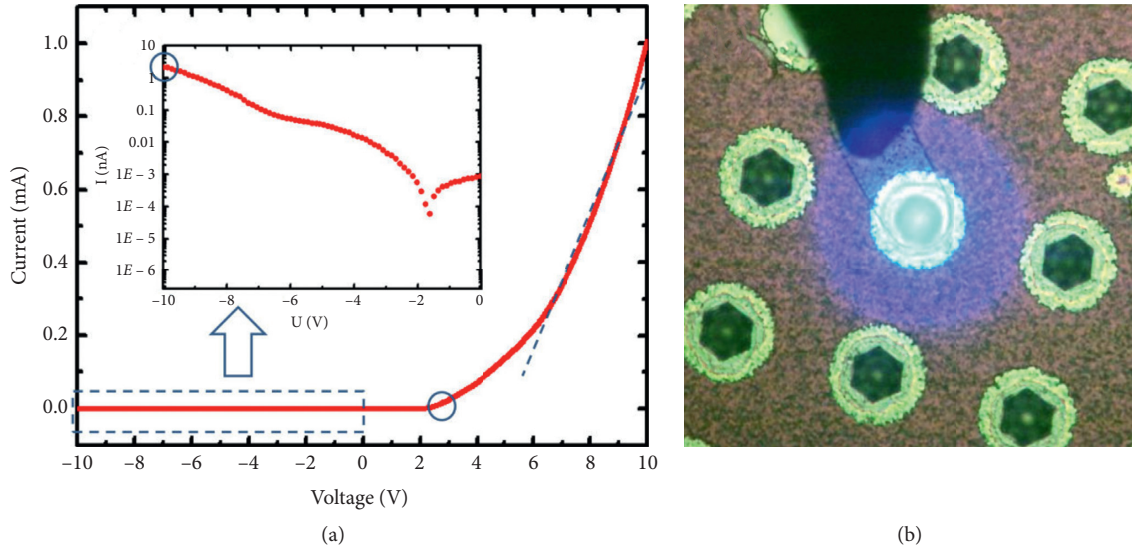


FIGURE 2: (a) I-V curve and (b) optical microscope photograph of micropyramid UV LED.

The detailed growth condition of the micropyramid LED in window areas are shown in Table 1.

The scanning electron microscopy (SEM) images of Figures 1(b) and 1(c) showed that the micropyramid of six semipolar planes were symmetrical and smooth. The bottom diameter ($20\ \mu\text{m}$) of the micropyramid was much larger than the window of the mask due to the lateral growth. The angle between $\{1\bar{1}01\}$ and (0001) crystal plane was 62° . A 250 nm thick indium tin oxide (ITO) film was deposited on the micropyramid LED as a transparent conducting layer (TCL), followed by the thermal annealing at 550°C for 30 min in nitrogen (N_2) environment. A Ti/AuSb/Au (10 nm/20 nm/200 nm) metal was stacked on n-type Si by E-beam evaporation and rapid thermal annealing at 380°C for 35 seconds in nitrogen (N_2) environment. More detailed structure is shown in Figure 1(a). In this way, the single electrically driven micropyramid vertical GaN-based UV LED was manufactured.

3. Results and Discussion

In order to study the electrical performance of micropyramid UV LED, the current-voltage (I-V) characteristic has been measured by Agilent B1500A, and the I-V curve is shown in Figure 2(a). The curve shows the I-V characteristic of a typical p-n junction due to the micropyramidal n-GaN/n-AlGaN and p-AlGaN/p-GaN layers. The turn-on voltage

and series resistance are $\sim 2.5\ \text{V}$ and $5.2 \times 10^3\ \Omega$, respectively. Series resistance of unit area is only a quarter of vertical LEDs [16]. This attribution virtually leads to the high optical output power. The doping in growth and high-quality ohmic contact results in a low resistance. The reverse leakage current of micropyramid UV LED is 2 nA at $-10\ \text{V}$. There are few reverse leakage current channels in micropyramid UV LEDs because the micropyramid n-GaN releases partial stress from the lattice mismatch and the dislocation density is low. The working photograph is shown in Figure 2(b), and the single micropyramid UV LED is located at the centre of the high brightness region.

Figure 3 shows the electroluminescence (EL) spectra of micropyramid UV LED working at various currents from 2 to 7 mA. The micropyramid UV LED has a high optical output intensity under a small current injection.

Under positive bias, electrons cross the AlGaN/GaN MQWs layer and recombine with holes in the p-GaN layer by radiative recombination. The EL curves show 365 nm and 386 nm emission peaks, which come from the emission of the GaN/AlGaN MQWs and the p-GaN layer [8], respectively. The peak of 386 nm is higher than the peak of 365 nm because the Al composition in the barrier of $\text{Al}_{0.06}\text{Ga}_{0.94}\text{N}/\text{GaN}$ MQWs is low and the p-GaN can absorb the 365 nm light [17].

The inset of Figure 3 shows the optical microscope photograph of the micropyramid UV LED when the injection current is 0.2 mA and 2 mA, respectively. The light of

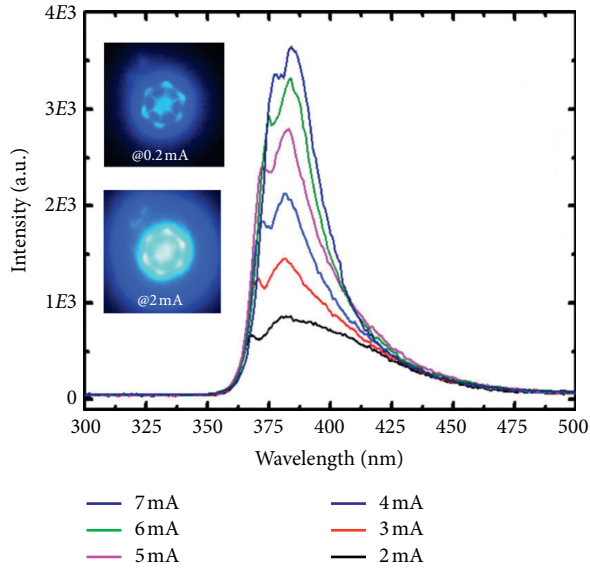


FIGURE 3: EL spectra of micropyramid UV LED working at various currents from 2 to 7 mA.

the micropyramid UV LED distributes on the top, six bottom corner and edges due to the high radiation recombination efficiency at the top of the pyramid [18–20]. The top of the pyramid is a high-brightness region due to the lower TDs, and the lower polarization effects and the larger emitting area of six semipolar planes. However, the bottom and six planes of the pyramid do not emit light at a low current due to the nonradiative recombination of the dislocation at the bottom and the 90° TDs at six planes of the pyramid. The light at the bottom and the six edges come from the emission of the top by waveguide of pyramid structure [21, 22]. As the injection current increases, the emission of top gradually spreads to the bottom.

In the EL spectra of micropyramid UV-LED, as shown in Figure 3, the peaks of the wavelengths of 365 nm and 386 nm show a red shift with increasing the injecting current. For an easier reference, the peak near the 365 nm and 386 nm is named as the first peak and the second peak, respectively. The relation between the peak positions and the injection current has been shown in Figure 4.

As shown in Figure 4, the wavelengths of two peaks increase with the strength of the injection current due to the heat effect of electric current.

In the temperature range of 200–800 K, the band gap of GaN can be expressed by the Varshni equation as follows [23, 24].

$$E_g(T) = E_g(0K) - \frac{\alpha T^2}{\beta + T}, \quad (1)$$

where $E_g(0K) = 3.495$ eV is the band gap of GaN at $T = 0K$; $\alpha = 0.94$ meV/K is the empirical constant; and $\beta = 791$ K is associated with the Debye temperature [24]. Equation (1) indicates the heat effect of electric current would result in the decrease of the band gap, which results in the red shift of the peaks in the EL spectra.

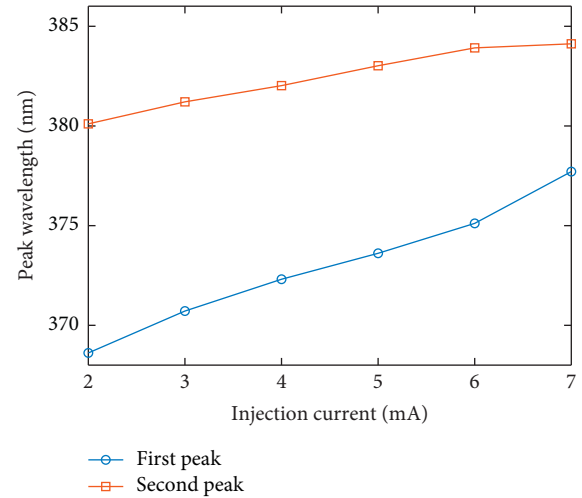


FIGURE 4: The relation between the positions of the first and second peaks and the injection current.

On the other hand, the state density of conduction band and the Fermi level increases with the strength of the injection current, and it would lead to the blue shift of the peaks in the EL spectra. The combined action of the two factors brings about the red shift of the peaks of the wavelengths of 365 nm and 386 nm.

4. Conclusion

In summary, micropyramid vertical GaN-based UV LED was fabricated on 2-inch n-Si (111) by SAG in a low-pressure MOCVD system. The top of the pyramid is the high-brightness region due to the lower TDs, the lower polarization effects, and the larger emitting area of six semipolar planes. However, no-light emission comes from the bottom and six planes of the pyramid at a low current due to the leakage current and nonradiative recombination of the dislocation at the bottom and the 90° TDs on six planes of the pyramid. The turn-on voltage, series resistance, and reverse leakage current of the single micropyramid UV LED are ~ 2.5 V, $5.2 \times 10^3 \Omega$, and 2 nA at -10 V, respectively. The series resistance of unit area is only a quarter of the conventional vertical LEDs, and the micropyramid UV LED has a high optical output intensity under a small current injection. It means the micropyramid UV LED can be used as a subminiature UV light source, and it would have a high output power under a small current injection. In addition, the reason why the peaks of the wavelengths of 365 nm and 386 nm in the EL spectra show a red shift with increasing the injecting current has been explained.

Data Availability

The data used to support the findings of this study are available from the corresponding author upon request.

Conflicts of Interest

The authors declare that they have no conflicts of interest.

Acknowledgments

The work was partially supported by the Key-Area Research and Development Program of Guangdong Province, China (Grant nos. 2019B010132001 and 2019B010132003), the joint funding of the Nature Science Foundation of China (NSFC) and the Macao Science and Technology Development Fund (FDCT) of China (Grant no. 62061160368), the National Key Research and Development Program (Grant nos. 2016YFB0400105 and 2017YFB0403001), and the Zhuhai Key Technology Laboratory of Wide Bandgap Semiconductor Power Electronics, Sun Yat-sen University, China (Grant no. 20167612042080001).

References

- [1] F. A. Ponce and D. P. Bour, "Nitride-based semiconductors for blue and green light-emitting devices," *Nature*, vol. 386, no. 6623, pp. 351–359, 1997.
- [2] I. Vurgaftman, J. R. Meyer, and L. R. Ram-Mohan, "Band parameters for III-V compound semiconductors and their alloys," *Journal of Applied Physics*, vol. 89, no. 11, pp. 5815–5875, 2001.
- [3] Y. Li, W. Wang, L. Huang et al., "High-performance vertical GaN-based near-ultraviolet light-emitting diodes on Si substrates," *Journal of Materials Chemistry C*, vol. 6, no. 42, pp. 11255–11260, 2018.
- [4] J.-T. Oh, Y.-T. Moon, D.-S. Kang et al., "High efficiency ultraviolet GaN-based vertical light emitting diodes on 6-inch sapphire substrate using ex-situ sputtered AlN nucleation layer," *Optics Express*, vol. 26, no. 5, pp. 5111–5117, 2018.
- [5] C. C. Li, J. L. Zhan, Z. Z. Chen et al., "Operating behavior of micro-LEDs on a GaN substrate at ultrahigh injection current densities," *Optics Express*, vol. 27, no. 16, pp. A1146–A1155, 2019.
- [6] Y. Muramoto, M. Kimura, and S. Nouda, "Development and future of ultraviolet light-emitting diodes: UV-LED will replace the UV lamp," *Semiconductor Science and Technology*, vol. 29, no. 8, p. 084004, 2014.
- [7] S. Xiao, T. Wang, T. Liu, C. Zhou, X. Jiang, and J. Zhang, "Active metamaterials and metadevices: a review," *Journal of Physics D: Applied Physics*, vol. 53, no. 50, p. 503002, 2020.
- [8] M. A. Reshchikov and H. Morkoç, "Luminescence properties of defects in GaN," *Journal of Applied Physics*, vol. 97, no. 6, p. 061301, 2005.
- [9] D. Zubia and S. D. Hersee, "Nanoheteroepitaxy: the Application of nanostructuring and substrate compliance to the heteroepitaxy of mismatched semiconductor materials," *Journal of Applied Physics*, vol. 85, no. 9, pp. 6492–6496, 1999.
- [10] H. Amano, N. Sawaki, I. Akasaki, and Y. Toyoda, "Metal-organic vapor phase epitaxial growth of a high quality GaN film using an AlN buffer layer," *Applied Physics Letters*, vol. 48, no. 5, pp. 353–355, 1986.
- [11] H. P. Zhao, G. Y. Liu, J. Zhang, J. D. Poplawsky, V. Dierolf, and N. Tansu, "Approaches for high internal quantum efficiency green InGaN light-emitting diodes with large overlap quantum wells," *Optics Express*, vol. 19, no. 14, pp. A991–A1007, 2011.
- [12] J. H. Ryou, P. D. Yoder, J. P. Liu et al., "Control of quantum-confined Stark effect in InGaN-based quantum wells," *IEEE Journal of Selected Topics in Quantum Electronics*, vol. 15, no. 4, pp. 1080–1091, 2009.
- [13] E. T. Yu, X. Z. Dang, P. M. Asbeck, S. S. Lau, and G. J. Sullivan, "Spontaneous and piezoelectric polarization effects in III-V nitride heterostructures," *Journal of Vacuum Science & Technology B: Microelectronics and Nanometer Structures*, vol. 17, no. 4, pp. 1742–1749, 1999.
- [14] J. Zhao, X. Zhang, J. He et al., "High internal quantum efficiency of nonpolar a-plane AlGaIn-based multiple quantum wells grown on r-plane sapphire substrate," *ACS Photonics*, vol. 5, no. 5, pp. 1903–1906, 2018.
- [15] S. Tanaka, Y. Kawaguchi, N. Sawaki, M. Hibino, and K. Hiramatsu, "Defect structure in selective area growth GaN pyramid on (111)Si substrate," *Applied Physics Letters*, vol. 76, no. 19, pp. 2701–2703, 2000.
- [16] Y. B. Yang, Y. Lin, P. Xiang et al., "Vertical-conducting InGaIn/GaN multiple quantum wells LEDs with AlN/GaN distributed Bragg reflectors on Si(111) substrate," *Applied Physics Express*, vol. 7, no. 4, p. 042102, 2014.
- [17] N. Otsuka, A. Tsujimura, Y. Hasegawa, G. Sugahara, M. Kume, and Y. Ban, "Room temperature 339 nm emission from Al_{0.13}Ga_{0.87}N/Al_{0.10}Ga_{0.90}N double heterostructure light-emitting diode on sapphire substrate," *Japanese Journal of Applied Physics*, vol. 39, no. 5B, pp. L445–L448, 2000.
- [18] B. Monemar, P. P. Paskov, J. P. Bergman et al., "Recombination of free and bound excitons in GaN," *Physica Status Solidi B*, vol. 245, no. 9, pp. 1723–1740, 2008.
- [19] L. Liu, L. Wang, C. Lu et al., "Enhancement of light-emission efficiency of ultraviolet InGaIn/GaN multiple quantum well light emitting diode with InGaIn underlying layer," *Applied Physics A*, vol. 108, no. 4, pp. 771–776, 2012.
- [20] A. E. Chernyakova, M. M. Soboleva, V. V. Ratnikova, N. M. Shmidta, and E. B. Yakimov, "Nonradiative recombination dynamics in InGaIn/GaN LED defect system," *Superlattices & Microstructures*, vol. 45, no. 4-5, pp. 301–307, 2009.
- [21] H. X. Jiang, J. Y. Lin, K. C. Zeng, and W. Yang, "Optical resonance modes in GaN pyramid microcavities," *Applied Physics Letters*, vol. 75, no. 6, pp. 763–765, 1999.
- [22] A. David, C. Meier, R. Sharma et al., "Photonic bands in two-dimensionally patterned multimode GaN waveguides for light extraction," *Applied Physics Letters*, vol. 87, no. 10, p. 101107, 2005.
- [23] N. M. Ravindra and V. K. Srivastava, "Temperature dependence of the energy gap in semiconductors," *Journal of Physics and Chemistry of Solids*, vol. 40, no. 10, pp. 791–793, 1979.
- [24] N. Nepal, J. Li, M. L. Nakarmi, J. Y. Lin, and H. X. Jiang, "Temperature and compositional dependence of the energy band gap of AlGaIn alloys," *Applied Physics Letters*, vol. 87, no. 24, p. 242104, 2005.